# Controlling the self-collimation characteristics of a near-infrared two-dimensional metallic photonic crystal*

Feng Shuai(冯 帅)[a)†], Ren Cheng(任 承)[b)], Wang Wen-Zhong(王文忠)[a)], and Wang Yi-Quan(王义全)[a)]

[a)] *School of Science, Minzu University of China, Beijing* 100081, *China*

[b)] *School of Opto-electronic Information Science and Technology, Yantai University, Yantai* 264005, *China*

(Received 3 February 2012; revised manuscript received 6 June 2012)

Self-collimation characteristics of the two-dimensional square-lattice photonic crystal (PC) consisting of metal rods immersed in silicon are studied by the finite-difference time-domain method. The Drude dispersion model is adopted to describe the metal rod, and the self-collimation behaviours of the near-infrared light through the PC are studied. The frequency region and the tolerance of incident angle for the self-collimation behaviour can be controlled by changing the shape of the metal rods.

**Keywords:** photonic crystal, self-collimation, beam splitter

**PACS:** 42.70.Qs, 78.20.Ci **DOI:** 10.1088/1674-1056/21/11/114212

## 1. Introduction

Photonic crystal (PC) has attracted a lot of attention owing to the existence of photonic band gaps, where light propagation is completely prohibited in any direction.[1,2] By creating different kinds of defects into a perfect PC, various photonic devices can be created, such as waveguides,[3−5] filters[6−9] and ultrafast optical switches.[10,11] In recent years, there has been a growing interest in anomalous dispersion properties of PC, such as negative refraction,[12,13] self-collimation,[14−19] and so on. The self-collimation phenomenon allows an incident light to propagate along a definite direction with almost no diffraction in a perfect PC. The advantage of the self-collimation-based device is that it requires neither a physical boundary for achieving the narrow lateral confinement nor a precise alignment for coupling into narrow waveguides. Many interesting devices have been designed based on the dispersion-based self-collimation effect, such as defect-free waveguides, beam splitters, polarization splitters, and so on.

Kosaka *et al.*[14] first demonstrated the self-collimated propagation of light in the PC experimentally; Lee *et al.*[15] showed that self-collimated beams can be easily bent and split by introducing line defects in the PC structures. In the last few years, a great deal of research work has been done to broaden the frequency region where the self-collimation phenomenon occurs,[16] to expand the incident angle range,[17] and to reduce the reflection on the interface.[18] Recently, Wu *et al.*[19] found that the all-angle broad-band self-collimation phenomenon exists in the two-dimensional (2D) rhombic-lattice PC consisting of silicon rods in air. The effects of the lattice angle and radius of the rod on the bandwidth of the self-collimation frequency region are investigated. In this paper, we study the 2D all-solid-type PC structure consisting of metallic rods immersed in a silicon background. It is shown that the frequency region and the tolerance of incident angles for self-collimation phenomena can be controlled by changing the shape of the metallic rod. The self-collimation frequency bandwidth and the transmission efficiency can be enhanced by increasing the metal side length along the light propagation direction.

## 2. Numerical simulation and discussion

The structure studied in this paper is based on a 2D square-lattice PC consisting of metallic rods im-

*Project supported by the National Natural Science Foundation of China (Grant Nos. 10904176, 11004169, and 11047127), the Doctoral Foundation of Shandong Province, China (Grant No. BS2009CL028), the "985 Project", China (Grant No. 98507-012009), and the "211 Project" of the Ministry of Education of China.

†Corresponding author. E-mail: fengshuai75@163.com

© 2012 Chinese Physical Society and IOP Publishing Ltd

mersed in silicon. The length of the PC lattice constant, denoted by $a$ in the following section, equals 400 nm and the refractive index of the background material is 3.45. The Drude dispersion model is adopted to describe the permittivity of the metal rod, which is given as

$$\varepsilon(\omega) = \varepsilon_0 \left(1 - \frac{\omega_{\rm p}^2}{\omega\,(\omega + {\rm i}\gamma)}\right),$$

where $\omega_{\rm p}$ is the plasma frequency, and $\gamma$ is the damping coefficient. The metal studied in this paper is Ag, and the corresponding values are $\omega_{\rm p} = 1.37 \times 10^{16}$ Hz and $\gamma = 2.73 \times 10^{13}$ Hz. For 2D PC, the electromagnetic waves can be separated into two independent polarized modes, the TM-polarized mode and TE-polarized mode. In this paper, we consider only the TM polarization mode, where the electric field $E_z$ is kept parallel to the extension axis of the metallic rod (assumed to be the $z$ axis). In all the simulations throughout this paper, we employ the finite-difference time-domain (FDTD) method with the periodic boundary condition to calculate the band structures and the equal-frequency surface contours (EFCs) in the reciprocal space, while Berenger's perfectly matched layer absorbing boundary condition is employed to calculate the wave propagation in the finite real space.[20,21] In all the simulations, the size of the lattice constant is divided into 30 lattice grids. For the frequencies centred at 0.26 $c/a$ ($c$ is the light velocity in a vacuum), which are studied in this paper, the size of the lattice grid is less than one percent of the central wavelength in a vacuum. This value is much less than the lattice grid's basic requirement of smaller than $\lambda/15$, and good accuracy is ensured.

At first, we adopt square metal rods to constitute a square-lattice PC structure. The side length of the metal is $l = 170$ nm. Ignoring the absorption of the metal to the light beams, the calculated band structures for several lowest photonic bands are shown in Fig. 1(a) for the TM-polarized modes. It can be seen that the metallic rods lift the first TM-polarized band and cause a stop band at the lowest frequencies. The cutoff frequency of this metallic PC is about 0.15 $c/a$. There is no band gap between the second and the third photonic bands.

It is well known that the propagation direction of light is identical to the direction of the group velocity of light given by $v_{\rm g} = \nabla_k \omega(k)$, which means that the group velocity is perpendicular to the EFC. Through an analysis of the EFC as a function of $k$, we can find the frequency range in which the self-collimation phenomenon occurs and the propagation direction of the light beam. Several EFCs in the second and third TM-polarized bands are shown in Figs. 1(b) and 1(c), respectively. It can be

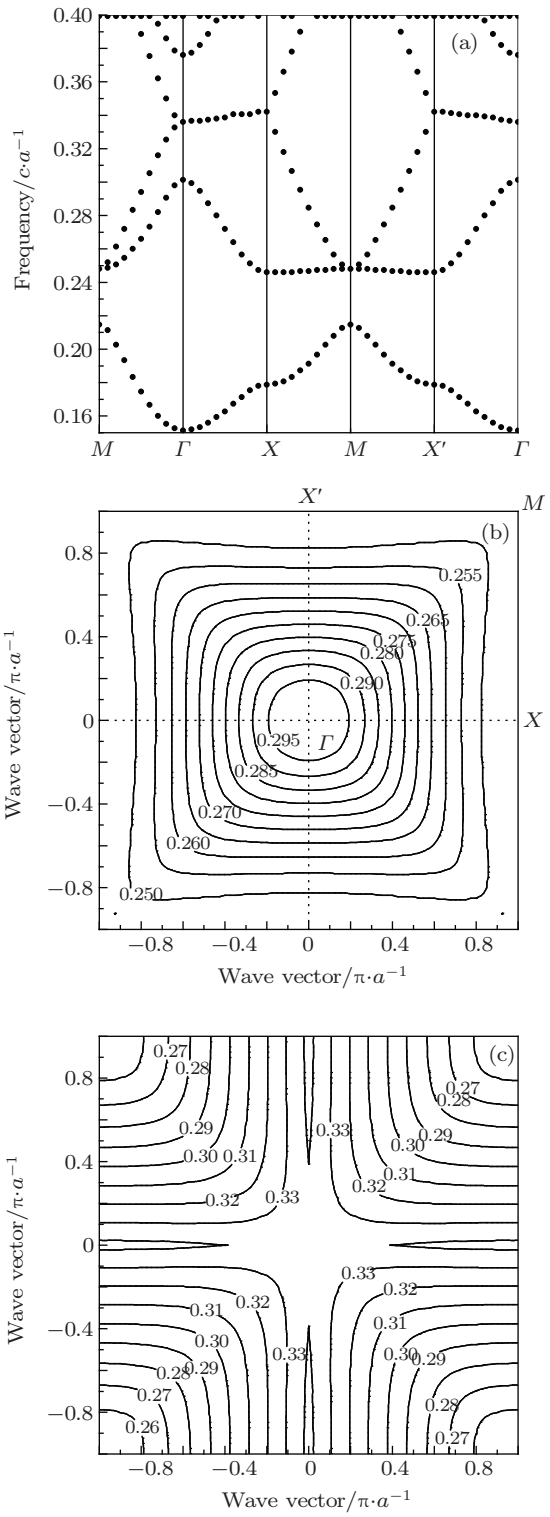



**Fig. 1.** (a) TM-polarized photonic band structure of the 2D square-lattice metallic PC, and the corresponding EFCs within the second (b) and the third (c) photonic bands.

seen from Fig. 1(b) that the EFCs around the frequency 0.26 $c/a$ (the corresponding wavelength in a vacuum is 1538 nm) are quite flat and have the surface normally pointing to the $\Gamma X$ direction. It means that the incident light at this frequency will propagate through the PC along the $\Gamma X$ direction. In the minor part of the curve around the $\Gamma M$ direction, the curve points towards the $\Gamma$ point; the radius of curvature reduces with an increase of the frequency, meaning an apparent negative refraction direction for the PC slab. When the light beam resonant at frequency 0.26 $c/a$ propagates through the PC structure with incident angles of 0° and 30°, whose sketch map is shown in Fig. 2(a), the steady spatial light intensity distributions through the metallic PC slab are calculated by the FDTD method; the results are shown in Figs. 2(b) and 2(c), respectively. It can be seen that good self-collimation behaviour occurs at normal incidence, and disappears when the incident angle is changed to 30°. The frequency region, in which the self-collimation phenomenon occurs at normal incidence, is calculated; it spans the frequencies 0.25 $c/a$ and 0.275 $c/a$.

To enlarge the frequency region in which the self-collimation phenomenon occurs, we change the shape of the metal from square to rectangle. Firstly, we set the side length of the rectangle along the light propagation to be 250 nm, and the other side length to be 130 nm. Figure 3(a) shows the photonic band structure of the above structure, from which we can see that the lowest photonic band is not sensitive to the change of the metal's shape, while the third photonic band moves upwards evidently. It can be seen from Fig. 3(b) that the EFCs around 0.26 $c/a$ are quite flat in the region centred on the $\Gamma X$ line, and its surface normal

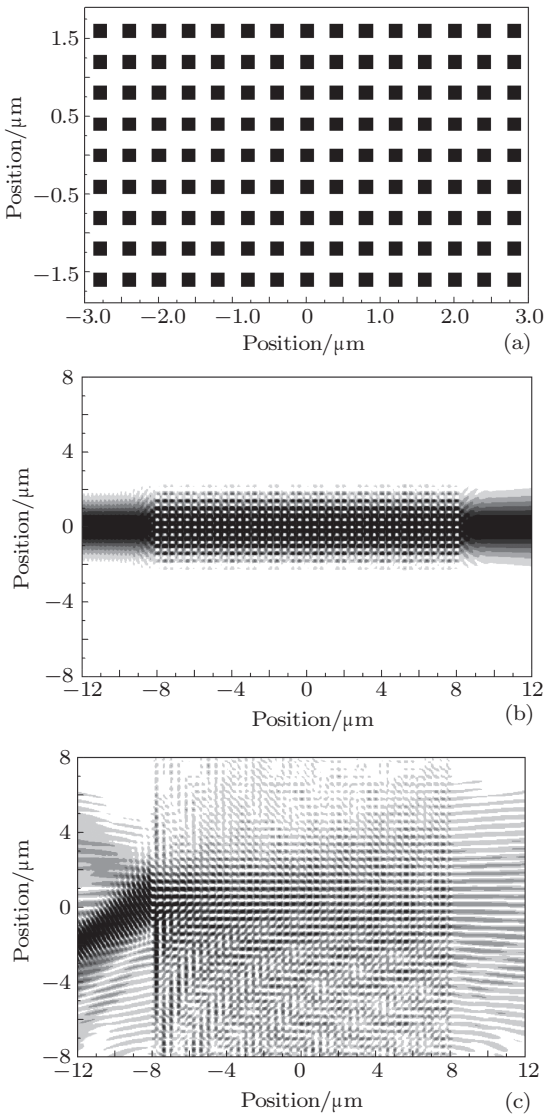



**Fig. 2.** (a) Structure of the metallic PC, and the spatial distributions of light intensity at the frequency 0.26 $c/a$ and the incident angles of (b) 0° and (c) 30°.

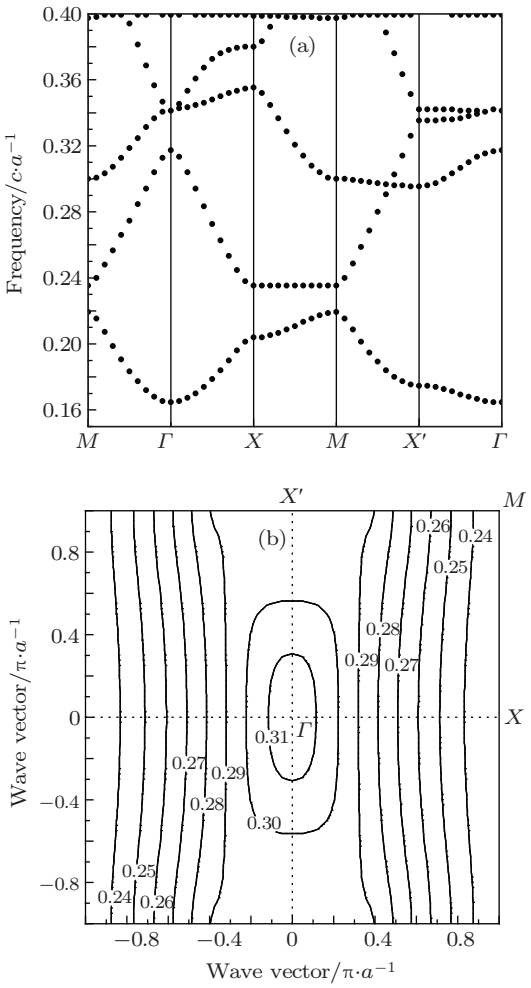



**Fig. 3.** (a) TM-polarized photonic band structure of the 2D square-lattice metallic PC, and (b) the corresponding EFCs within the second band.

points to the $\Gamma X$ direction, meaning that good self-collimation behaviour occurs along the $\Gamma X$ direction. When the wave vector of 0.26 departs from the $\Gamma X$ line and is located around the $\Gamma$ direction, the corresponding EFC's surface normally points to a negative refractive direction, which can be deduced by analyzing the radius of EFC's curvature reducing with the increase.

Figure 4(a) shows the sketch map of the above PC structure consisting of rectangular metals. When a light beam resonant at frequency 0.26 $c/a$ propagates through the PC structure at the incident angles of 0°, 30°, and 45°, the light intensity spatial distributions across the metallic PC slab are shown in Figs. 4(b)–4(d), respectively. It can be seen that good self-collimation behaviour occurs at the normal incidence. When the incident angle is 30°, good self-collimation behaviour occurs inside the PC, and two output light beams are obtained at the other side of the PC. The direction of one output light beam is parallel to that of the incident light beam, which can be easily understood by the law of refraction. The light beam points to a negative-refraction direction, which is formed by the collective action of the parallel subwavelength-width light beams at the right side of the PC boundary. Figure 4(d) shows that the self-collimation direction deviates from the $\Gamma X$ direction of the PC when the incident angle is changed into 45°, which can be understood by analyzing the shape of the EFC. The frequency region, in which the self-collimation phenomenon occurs at the normal incidence in this kind of PC structure, is from 0.24 $c/a$ to 0.3 $c/a$.

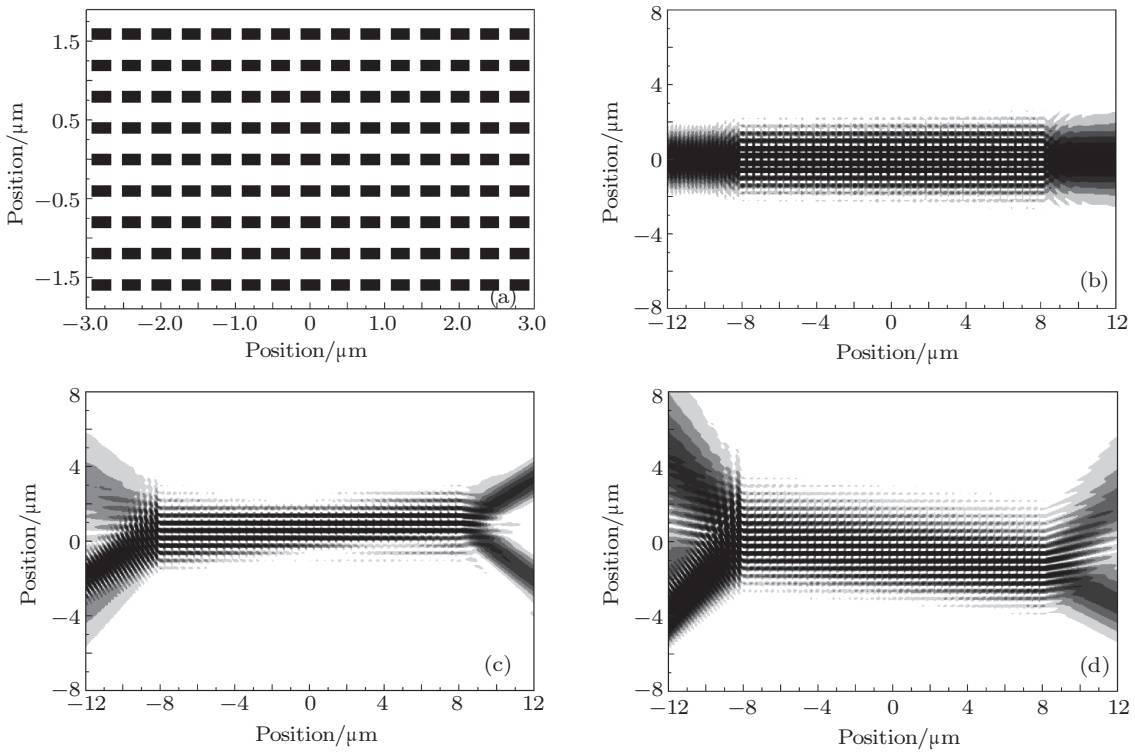



**Fig. 4.** (a) Structure of the metallic PC, and the spatial distributions of light intensity at the frequency 0.26 $c/a$ and the incident angles of (b) 0°, (c) 30° , and (d) 45°.

Finally, we changed the side length of the rectangle along the light propagation to 330 nm, and the other side length to 90 nm. Figure 5 shows the photonic band structure of the above structure and several EFCs in the second band. Comparing Fig. 5 with Fig. 3, the third photonic band moves upwards further for a certain degree. And the EFCs in the whole second band are almost perfectly flat with the normal surface pointing to the $\Gamma X$ direction, meaning that all-angle self-collimation behaviour occurs regardless of the size of the corresponding EFC in air. This all-angle self-collimation frequency region is from 0.22 $c/a$ to 0.31 $c/a$. The relative bandwidth of this region is about 34% of the central frequency.

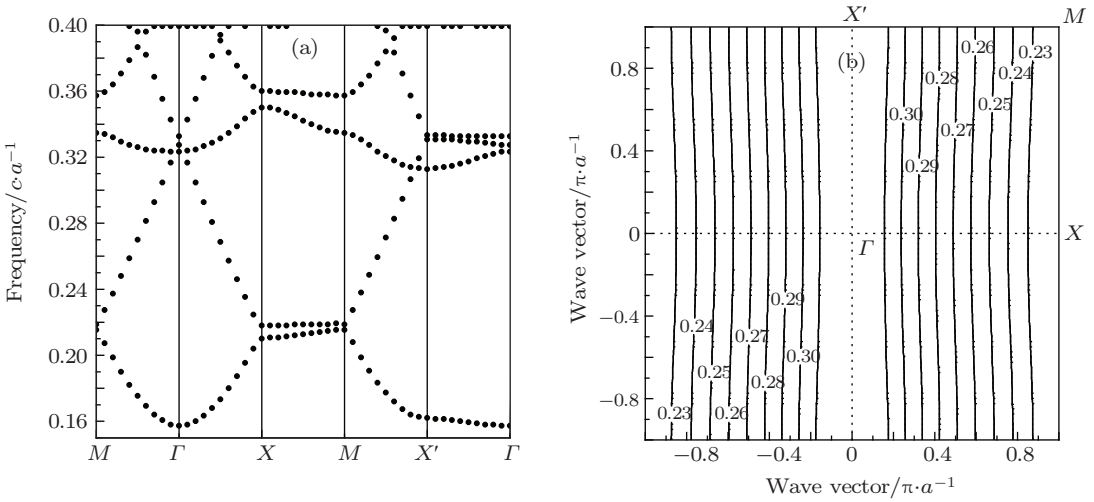



**Fig. 5.** (a) TM-polarized photonic band structure of the 2D square-lattice metallic PC and (b) the correponding EFCs within the second band.

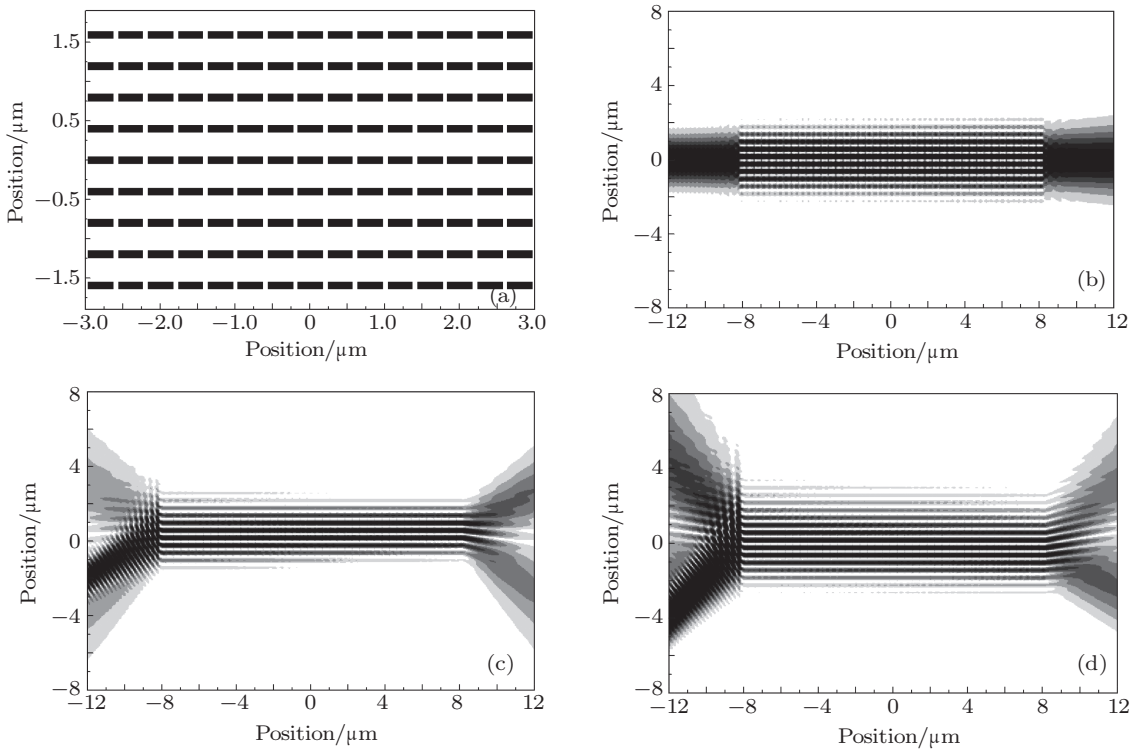



**Fig. 6.** (a) Structure of the metallic PC, and the spatial distributions of light intensity at the frequency 0.26 $c/a$ and the incident angles of (b) 0°, (c) 30°, and (d) 45°.

When the light beam at 0.26 $c/a$ propagates through the PC structure shown in Fig. 6(a) at the incident angles of 0°, 30°, and 45°, the corresponding steady light intensity spatial distributions across the metallic PC are shown in Figs. 6(b)–6(d), respectively. It is shown that good self-collimation behaviour along the $\Gamma X$ direction occurs in all the incident angles. When the light beam is not at the normal incidence, two output light beams are obtained through the PC.

Figure 7 shows the calculated light transmittance through the above 16 μm-thick PC slab at the normal incidence. The dashed line $a$ corresponds to the structure shown in Fig. 2(a), the dotted line $b$ corresponds to the structure displayed in Fig. 4(a), and the solid line $c$ corresponds to the structure indicated in Fig. 6(a). Owing to the convenience of our calculation, the areas of the above three metal rods may not be exactly the same. The difference between their ar-

eas is trivial for influencing the self-collimation working frequencies. It can be seen that the central frequencies, where the self-collimation behaviour occurs, are almost the same. It was found that the high-transmittance frequency region can be enlarged by increasing the rectangle side length along the $\Gamma X$ direction of the PC. At the same time, the light transmission efficiency can also be further enhanced. The light transmittances through the same PC structure at different incident angles are also calculated. Owing to the decrease of the light intensity component in the self-collimation direction, the light transmittance reduces with the increase of the incident angle. And the corresponding values are of the same order of magnitude on the condition that the incident angle is not very large.

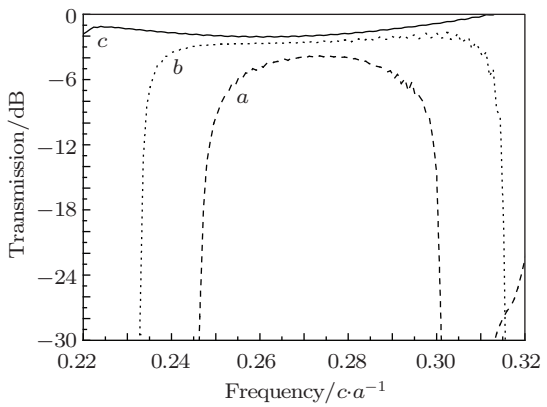



**Fig. 7.** Light transmittances at normal incidence through the 41-rod-thick PC structures shown in Figs. 2, 4, and 6, which are shown by the dashed ($a$), dotted ($b$), and solid ($c$) lines, respectively.

## 3. Conclusions

The self-collimation characteristics of 2D near-infrared metallic PC are studied. The frequency region and the tolerance of incident angle for self-collimation behaviour can be adjusted by changing the size of the rectangular metal. The light propagating direction within the PC region can tolerate a change of the incident angle within a certain region. When the light is not at normal incidence, two output light beams can be obtained through the PC, while the light beam travels within the PC in the same direction. The absorption of metal rods can be further reduced by lessening the width of the rectangular metal vertical to the light transmission. Our designed structures provide the evidence for the intriguing potential of self-collimated beams as a basis for integrated photonic circuits.

## References

[1] Yablonovitch E 1987 *Phys. Rev. Lett.* **58** 2059
[2] John S 1987 *Phys. Rev. Lett.* **58** 2486
[3] Johnson S G, Villeneuve P R, Fan S and Joannopoulos J D 2000 *Phys. Rev.* B **62** 8212
[4] Tokushima M and Yamada H 2002 *IEEE J. Quantum Elect.* **38** 753
[5] Feng S and Wang Y Q 2011 *Chin. Phys.* B **20** 054209
[6] Fan S, Villeneuve P R, Joannopoulos J D and Haus H A 1998 *Phys. Rev. Lett.* **80** 960
[7] Takano H, Akahane Y, Asano T and Noda S 2004 *Appl. Phys. Lett.* **84** 2226
[8] Liu J T, Zhou Y S, Wang F H and Gu B Y 2005 *Chin. Phys.* **14** 2474
[9] Feng S and Wang Y Q 2011 *Chin. Phys.* B **20** 104207
[10] Villeneuve P R, Abrams D S, Fan S and Joannopoulos J D 1996 *Opt. Lett.* **21** 2017
[11] Hu X Y, Liu Y H, Tie J, Cheng B Y and Zhang D Z 2005 *Appl. Phys. Lett.* **86** 121102
[12] Kosaka H, Kawashima T, Tomita A, Notomi M, Tamamura T, Sato T and Kawakami S 1998 *Phys. Rev.* B **58** R10096
[13] Parimi P V, Lu W T, Vodo P, Sokoloff J, Derov J S and Sridhar S 2004 *Phys. Rev. Lett.* **92** 74011
[14] Kosaka H, Kawashima T, Tomita A, Notomi M, Tamamura T, Sato T and Kawakami S 1999 *Appl. Phys. Lett.* **74** 1212
[15] Lee S G, Oh S S, Kim J E and Parka H Y 2005 *Appl. Phys. Lett.* **87** 181106
[16] Hamam R E, Ibanescu M, Johnson S G, Joannopoulos J D and Soljacic M 2009 *Opt. Express* **17** 8109
[17] Botten L C, White T P, de Sterke C M and McPhedran R C 2006 *Phys. Rev.* E **74** 026603
[18] Lawrence F J, Botten L C, Dossou K B and de Sterke C M 2008 *Appl. Phys. Lett.* **93** 1114
[19] Wu Z H, Xie K, Yang H J, Jiang P and He X J 2012 *J. Opt.* **14** 015002
[20] Yee K S 1966 *IEEE Trans. Antennas Propag.* **14** 302
[21] Berenger J P 1996 *J. Comput. Phys.* **127** 363